

Chronic NMDA Receptor Blockade From Birth Delays the Maturation of NMDA Currents, but Does Not Affect AMPA/Kainate Currents

MATTHEW T. COLONNESE,^{1,2} JIAN SHI,¹ AND MARTHA CONSTANTINE-PATON¹

¹Department of Biology, Department of Brain and Cognitive Science, and McGovern Institute for Brain Research, Massachusetts Institute of Technology, Cambridge, Massachusetts 02139; and ²Interdepartmental Neuroscience Program, Yale University, New Haven, Connecticut 06520

Submitted 25 January 2002; accepted in final form 11 September 2002

Colonnese, Matthew, T., Jian Shi, and Martha Constantine-Paton. Chronic NMDA receptor blockade from birth delays the maturation of NMDA currents, but does not affect AMPA/kainate currents. *J Neurophysiol* 89: 57–68, 2003; 10.1152/jn.00049.2002. The activity of the *N*-methyl-D-aspartate receptor (NR) regulates the composition of excitatory synapses and mediates multiple forms of synaptic and structural plasticity. In the superficial superior colliculus (sSC) of the rat, NR activity is essential for the full refinement of retinotopy during development. We have examined the NR's role in synaptic development by chronically treating the sSC from birth with the competitive antagonist (\pm)-2-amino-5-phosphonopentanoic acid (AP5) released by the slow-release polymer Elvax. Whole-cell voltage-clamp recordings were used to characterize excitatory postsynaptic potentials (EPSCs) in slices from postnatal day (P)12–20 sSC. Chronic NR blockade reduced the ratio of AMPA/kainate receptor (AMPA) to NR peak current amplitudes of both spontaneous (s)EPSCs and evoked EPSCs. Spontaneous NR current amplitude was increased following treatment, while spontaneous AMPAR currents were identical to those of controls, indicating that the ratio change was due to an increased NR current. Comparison of sEPSC frequency, AMPAR current rectification, and quantitative Western blots indicated that the characteristics of AMPARs at the synapse are normal following AP5 treatment. In the sSC, NR currents show a rapid decrease in decay time on P11 and previous studies in slices indicate this change results from a NR-mediated activation of the phosphatase calcineurin. Consistent with this *in vitro* finding, the down-regulation failed to occur in sSC chronically treated with AP5 *in vivo*. Together the present data show that NR function is necessary for subsequent NR current regulation *in vivo*, but it is not essential for the developmental expression of normal AMPAR currents.

INTRODUCTION

The *N*-methyl-D-aspartate receptor (NR) is a critical component of numerous forms of synaptic plasticity that organize the developing nervous system (Cline and Constantine-Paton 1989; Fox et al. 1996; Hahm et al. 1991; Iwasato et al. 1997; Simon et al. 1992). It has been proposed that NRs function as Hebbian coincidence detectors, specifically strengthening the synapses between coactive neurons and weakening the rest (for review see Constantine-Paton et al. 1990). Recent work has

indicated that NR function alters the architecture of the postsynaptic density by inserting and removing AMPA receptors (Carroll et al. 1999; Heynen et al. 2000; Shi et al. 1999; Zhu et al. 2000) and thereby alters the strength and stability of developing connections. In some cases current flow specifically through the NR will, in turn, modify NR current kinetics and subunit composition (Quinlan et al. 1999; Shi et al. 2000).

Despite the critical importance of the NR in synaptic development, there has been little examination of the synaptic currents of animals raised with altered NR currents during a major period of synaptogenesis and maturation. In previous work our laboratory has characterized the development of NR and AMPA/kainate receptor (AMPA) currents in the developing rat superficial superior colliculus (sSC). In this neuropil synaptic NR currents down-regulate their decay times during the second and third postnatal week. This down-regulation is the result of two processes, one fast and one gradual (Shi et al. 1997, 2000). The fast down-regulation occurs on postnatal day (P)11 and is the result of the persistent activation of the calcium-dependent phosphatase calcineurin. The second, gradual down-regulation occurs over the second and third postnatal weeks and appears to be due to the gradual incorporation of the NR2A subunit into synaptic NRs. We have also previously demonstrated that NRs can exert a substantial effect on AMPAR current development: low-level activation of NRs with a chronically applied agonist severely stalls synaptic maturation in the sSC, apparently by suppressing the normal expression of functional AMPAR at young contacts (Shi et al. 2001).

In the present paper we present the converse group of experiments. We have examined whether the NR is critical to the functional maturation of glutamatergic synapses *in vivo*, by chronically blocking sSC NRs with the competitive antagonist (D/L) AP5 released from Elvax implanted over the colliculus at birth. Whole-cell patch-clamping in slices was used to examine spontaneous and evoked postsynaptic currents in neurons that had developed under the AP5-Elvax treatment or under an Elvax-control releasing the inactive isomer L-AP5. Blockade did not perturb the development of AMPAR currents in any respect that we could identify. However, the fast down-regu-

Address for reprint requests: M. Constantine-Paton, Building 68-380, Massachusetts Institute of Technology, 77 Massachusetts Avenue, Cambridge, MA 02139-4307 (E-mail: mcpaton@mit.edu).

The costs of publication of this article were defrayed in part by the payment of page charges. The article must therefore be hereby marked "advertisement" in accordance with 18 U.S.C. Section 1734 solely to indicate this fact.

lation of NR decay time did not occur, resulting in NR currents that were much longer than those of control animals. In addition to the decay time, the amplitude of the NR current was also increased. These data indicate that current flow through the NR is a critical component in the developmental regulation of its own activity. They also suggest, however, that, in the sSC, NR function is not essential for AMPAR currents to attain their normal frequency, amplitude, and low Ca^{2+} permeability.

METHODS

Animals and materials

Timed pregnant Sprague–Dawley rats were acquired from CAMM Lab Animals (Wayne, NJ) or Charles River Breeding Laboratories (Willimington, MA) and housed in a 12/12 light/dark cycle. To chronically block NRs, the inert ethylene-vinyl acetate copolymer Elvax-40W (Dupont) was prepared as described (Prusky and Ramoa 1999; Simon et al. 1992). A 1-mM solution of the racemic mixture (D/L) AP5 (Sigma), or, as a control, a 500- μM solution of the inactive isomer L-2-amino-5-phosphopentanoic acid (L-AP5), was prepared in a solution of 10% Elvax in methylene chloride. The solvent was evaporated at -20°C and the resulting plugs were lyophilized overnight before being cut at 180 μm on a cryostat.

Surgery

All animal work was in accord with the provisions of the MIT ACUC. Elvax slabs were implanted at P0 using the method of Simon et al. (1992). Anesthesia was induced by hypothermia. The scalp was retracted and the skull and underlying dura were cut to allow a small sliver of Elvax to be inserted over the sSC with the front edge tucked under the occipital cortex. Sutures and tissue adhesive (Vetbond, 3M Animal Care Products) were used to close the incision, and the pups were warmed under a lamp until ready to be returned to the mother. Elvax releases water-soluble drug in the range of picomoles per day (Cline and Constantine-Paton 1989; Smith et al. 1995). Because the rate of clearance is unknown, the actual concentration in tissue is difficult to estimate. Recordings under the Elvax *in vivo* have demonstrated substantial blockade of all glutamateric activity (which occurs at $>500 \mu\text{M}$) when the concentration of D-AP5 in Elvax is 20 times ours (Schlaggar et al. 1993). Thus the concentration of D-AP5 in the sSC, which is $<200 \mu\text{M}$ from the surface, should conservatively be above 25 μM at all times during the treatment. In the first few days after implantation, levels will be higher ($>100 \mu\text{M}$) due to rapid release from the Elvax surface (Cline and Constantine-Paton 1989). One should keep in mind that these estimates are based on recordings under recently placed Elvax slabs, and the actual dynamics of release after chronic implantation can be unpredictable (Wallace et al. 2001). Nevertheless the concentration of AP5 and L-AP5 in Elvax used here is identical to that used in Colonnese and Constantine-Paton (2001), which showed reproducible alterations of axon sprouting in the sSC with AP5 treatment.

Electrophysiology

P12 to P20 pups were anesthetized with isoflurane and killed by decapitation. Only pups with no visible necrosis in the sSC were used for electrophysiological or biochemical analysis. The diencephalon and midbrain were placed in cold artificial cerebral spinal fluid (ACSF) containing (in mM) 117 NaCl, 3 MgCl_2 , 4 KCl, 3 CaCl_2 , 1.2 NaHPO_4 , 26 NaHCO_3 , and 16 glucose, saturated with 95% O_2 –5% CO_2 to a final pH of 7.4, and cut on a vibratome. ACSF was supplemented with 2 μM bicuculline methiodide (BMI) during recording unless otherwise indicated. Recordings were made from 300- to 400- μm parasagittal slices of the midbrain maintained at room

temperature (22 – 24°C) and perfused with ACSF at 4 ml/min. At least 2 h elapsed between cutting and recording from the slices. Recording procedures have been presented previously (Shi et al. 1997). Borosilicate glass (World Precision Instruments) patch electrodes with tip resistances of 5–10 $\text{M}\Omega$ were filled with (in mM) 122.5 Cs-gluconate, 17.5 CsCl, 10 HEPES (CsOH), 0.2 NaEGTA, 2 MgATP, 0.3 NaGTP, and 8 NaCl. In most experiments, 0.2% biocytin at pH 7.3 was added to the electrode to allow subsequent visualization of cell types. We have measured the liquid junction potential between the bath and electrode solution at between 9 and 10 mV (Shi et al. 1997). To compensate for this, an estimated offset of 10 mV has been added to all reported voltages. Cells had resting potentials between -45 and -58 mV.

Whole-cell recordings were restricted to neurons in the stratum griseum superficiale. All data included in this report are from recordings with seal resistances of 2–2.5 $\text{G}\Omega$ and series resistances of $<21 \text{M}\Omega$; neither changed more than 10% over the course of the experiment. Signals were recorded using an Axoclamp ID patch clamp amplifier, filtered at 5 kHz and interfaced (CED 1401 Plus, Cambridge Electronic Design) with a Pentium-based computer that stored the data and provided on-line response display and off-line data analysis. CED patch- and voltage-clamp software was used to acquire and analyze data.

Most of this analysis focused on spontaneous excitatory postsynaptic currents (sEPSCs) of cells held at -70 mV in 0 mM Mg^{2+} . Events were considered synaptic currents if they had rise times < 8 ms and amplitudes—measured from the noise midline—that were ≥ 2 times baseline noise (one-half the peak-to-peak amplitude, about 2 pA). Frequencies of EPSCs for each cell were obtained by randomly selecting intervals of ≥ 70 s, starting 2–3 min after setting the holding potential, and ≥ 5 min after a solution change. We counted all single fast currents meeting our criteria as synaptic currents within that interval. When multiple events were superimposed, later events were counted only when they occurred after the previous current had returned to $<20\%$ of peak value. This criterion was chosen for consistency with previous data analyses (Shi et al. 1997). Cells were analyzed only if their NR currents fully recovered following AP5 washout, and sEPSC amplitudes returned to within 20% of their initial values.

Currents from each neuron were averaged using customized software written by J.S. For comparison of decay kinetics across ages and treatments, we estimated the sEPSC decay time for each neuron using the cell's average sEPSC during the 70-s sample period and the single exponential τ estimator: time from peak to 0.37 peak amplitude. Averages were generally derived from ≥ 30 single events. For each neuron, sEPSCs were averaged before and again after the addition of 50 μM AP5. An estimate of the average NR current amplitude and decay for each neuron was obtained by subtracting the average sEPSC with AP5 from that without AP5 and measuring the calculated difference current. This technique was used to initially describe the rapid down-regulation of the NR current decay time (Shi et al. 1997), and subsequent work pharmacologically isolating NR currents (Shi et al. 2000) has shown that these subtraction currents are similar both in kinetics and amplitude to directly measured NR currents. This method of difference current analysis allowed for rapid data accumulation from each neuron because only the acutely applied AP5 had to be washed out of the tissue, minimizing the time in which the neurons could recover from the chronic treatment. We confirmed that substantial recovery from the chronic AP5 treatment did not occur during incubation and recording by maintaining several slices in perfusate supplemented with AP5 during the entirety of the cutting, recovery, and recording period. Data from these slices were indistinguishable from slices prepared without the continuous presence of AP5.

Electrical stimuli were delivered to the stratum opticum through bipolar electrodes composed of a pair of tungsten or platinum iridium microelectrodes with a tip separation of approximately 50 μm . Stimuli for the evoked currents consisted of 6- to 10- μA pulses of 0.5-ms

duration delivered at 0.1 Hz. The stimulation intensity for each cell was chosen to be roughly halfway between the minimal stimulation required to evoke a response and the point at which the response became saturated. Evoked currents were recorded in ACSF containing 2 mM Mg^{2+} and 6 μM BMI. The AMPAR contribution to the evoked EPSCs was determined at -70 mV in the presence of 100 μM AP5, and the NR contribution to these EPSCs was determined at $+40$ mV in the presence of 15 μM GYKI 52466, an AMPA/Kainate antagonist. Synaptic currents could be completely eliminated in the presence of all three drugs. Nine or more evoked currents at each holding potential were averaged for each neuron, and the average amplitude was used to determine AMPAR/NR peak current amplitude ratios. Again, only cells that maintained current amplitudes within 20% of initial baseline following washout of drugs were included for analysis.

AMPA current rectification experiments were the same as described above for AMPAR/NR current ratios, with a few exceptions. The ACSF was supplemented with 25 μM AP5, and the slices remained in this at all times. The internal pipette solution was supplemented with 0.1 mM spermine (Liu and Cull-Candy 2000) (Tocris). The baseline current amplitude was established at -70 mV. Current-voltage curves were generated from measurements taken at -70 , -40 , -20 , 0 , 20 , and 40 mV in random order, with four currents (<1 Hz) evoked at each holding potential. Measurements were again taken at -70 mV to ensure no fatigue had occurred.

Our recordings focused on the week after eye opening (P13), with most data points taken between P13 and P18. A few recordings were taken on P12 and P19–20 to see if there were large changes that occurred on these days. The period after eye opening was chosen for analysis for a number of reasons. First, we wished to address the specific question of whether AMPAR and/or NR currents are altered by developing in the absence of NR activity. There is substantial evidence that biochemical and anatomical changes occur in the rodent visual pathway in the short period following eye opening (Chen and Regehr 2000; Quinlan et al. 1999; Shi et al. 1997). Thus we thought that the sSC synapses might show the largest changes resulting from NR blockade during this time. This restricted focus renders it impossible to accurately extrapolate to potential disruption earlier or later in development. More comprehensive descriptions of the normal developmental sequence have been reported previously (Shi et al. 1997 2000) or are still underway (W. Liu, personal communication).

All pair-wise statistics are by 1-tailed Student's *t*-test (Microsoft Excel); the analysis of decay time changes with age and treatment were done by multivariate ANOVA followed by the Tukey posthoc test for pair-wise differences (Systat). Averages are \pm SE.

Western blotting

For biochemical experiments, rats were killed by carbon dioxide followed by cervical dislocation, and the sSC was rapidly dissected. Glutamate receptor and associated proteins were analyzed in both whole lysates and synaptoneurosomes fractions using previously published techniques (Hollingsworth et al. 1985; Scheetz et al. 2000). For these experiments single litters were divided into two groups, AP5 treated and their L-AP5 control littermates. The pups from each group were pooled during homogenization. Thus each litter contained two protein isolations, one treated and one control. Pups were killed at P12 (2 litters) or P16 (3 litters). The tissue was homogenized in ice-cold oxygenated buffer (in mM: 118 NaCl, 4.7 KCl, 1.2 $MgSO_4$, 2.5 $CaCl_2$, 1.53 KH_2PO_4 , and 5.25 sucrose) containing Complete Protease Inhibitor (Boehringer-Mannheim). For whole lysates, SDS was added to a fraction of the homogenate to a final concentration of 1% and solution was stored on ice. To make the synaptoneurosomes, the remainder of the homogenate was passed through a series of nylon filters of descending pore size (final pass through a MLCWP 047 Millipore filter with a 10- μm pore size) and centrifuged for 15 min at 1,000g. The pellet was resuspended in 1% SDS. Protein concentration was determined for all samples, which were then brought to 0.4 mg/ml

in Lamelli buffer. Aliquots were stored at $-80^\circ C$ until needed and were heated to $95^\circ C$ for 5 min before loading. Electrophoresis used 4–12% gradient polyacrylamide minigels (BioWhittaker) with 1.2–2.0 μg protein per lane. Proteins were transferred to nitrocellulose by electroblotting (Idea Scientific). Blots were blocked with 5% dried milk in 0.1% Tween and 0.1 M phosphate-buffered saline (TPBS), and incubated in primary antibody in TPBS. Protein bands were visualized by chemiluminescence and exposure to film.

Immunoblotting of proteins used primary antibodies to AMPAR subunits (GluR1, 1:1000 and GluR2, 1:1000; Chemicon), NR subunits (NR1, 1:1000, PharMingen; NR2A 1:500, Upstate Biologicals; NR2B, 1:300, Transduction Laboratories), PSD-95 (Clone K28/43 1:1000, Upstate Biologicals), pan-cadherin (1:1000, Zymed), NCAM (AG, 1:10, Developmental Hybridoma Bank), calcineurin α (1:1000, Sigma), β -catenin (1:1000, Sigma), β_3 integrin (1:1000, Pharmingen), and EphB2 (1:1000, gift of M.E. Greenberg, Harvard Medical School). An actin band blotted with antibody AC-40 (1:2000, Sigma) served as a loading control for each lane.

For quantification of Western blotting, band density was measured on two to four autoradiographs per paired protein isolation (2 for P12, 3 for P16) by densitometry using National Institutes of Health Image and gel plotting macros. Pixel intensities were calibrated to optical densities with a density wedge. Measurements were confirmed to be within the linear range by analysis of a dilution series with the samples. Each synaptic protein's densitometry measurement was normalized to its associated actin loading control. The change in protein density following AP5 treatment was calculated from the normalized bands of protein from control and treated littermates run out on the same gel. The normalized density for each lane of AP5-treated tissue was subtracted from the normalized density of band for the associated control L-AP5-treated littermate. This number was then divided by the same L-AP5 normalized density to determine the percentage of change. Thus the formula for each pair of bands was

Percent change in optical density

$$= (\text{SynD}_{\text{AP5}}/\text{ActinD}_{\text{AP5}} - \text{SynD}_{\text{control}}/\text{ActinD}_{\text{control}})/(\text{SynD}_{\text{control}}/\text{ActinD}_{\text{control}})$$

where SynD is the optical density of the synaptic protein of interest and ActinD is the optical density of the associated actin band. The final numbers were expressed \pm the 95% confidence interval for all the measurements made.

RESULTS

To examine the role of NRs in the development of sSC glutamatergic development we used the slow-release plastic Elvax to release the competitive antagonist AP5. The Elvax was placed above the sSC on the day of birth and remained there until the animals were killed for recording. Half of the animals of each individual litter received Elvax containing AP5, while the other half received Elvax with only with the inactive isomer L-AP5 as a control.

Previous work has indicated an activity-dependent down-regulation of the NR current decay time that occurs on P11 in the sSC (Shi et al. 1997). This down-regulation reduces the decay time of the spontaneous NR EPSC from between 20 and 25 ms to between 10 and 15 ms (Shi et al. 2000). We therefore performed all recordings on days P12–20, after this fast receptor down-regulation would normally have occurred. When quantitatively measuring the effect of the AP5 treatment we eliminated possible confounds of eye opening on the results by only including pups with open eyes (P13 and P20).

Reduced AMPAR/NR current ratio following NR blockade

To examine the effect of NR blockade on the development of the glutamate synapses made by the primary sSC afferents, EPSCs were evoked by stimulation of the stratum opticum at the rostral edge of the sSC. The slices were maintained in normal ACSF supplemented with BMI to block GABA_A receptors. AMPAR or NR currents were sequentially isolated pharmacologically by maintaining the neuron at -70 mV with

AP5 in the perfusate to examine AMPAR currents and by holding at $+40$ mV with GYKI in the perfusate to examine NR currents.

NR and AMPAR currents of neurons from AP5- and control (L-AP5)-treated colliculi were within the same amplitude range and were qualitatively similar to untreated sSC of the same age (Fig. 1A) (Shi et al. 1997).

To quantitatively examine the relative amplitudes of the evoked EPSCs we generated a ratio of the peak amplitude of the AMPAR and NR currents for each neuron (Fig. 1B). Such a ratio is necessary because the intensity of stimulation must vary between individual slices, making comparison of the absolute current amplitudes difficult. With one exception, all AP5-treated neurons examined had a lower AMPAR/NR current amplitude ratio than that of their age-matched controls (Fig. 1B). The average peak amplitude ratio of evoked current in neurons taken from P13 to P19 slices ($n = 12$ cells from 10 L-AP5 colliculi, and 15 cells from 9 AP5 colliculi) was 1.90 ± 0.20 for the L-AP5 group and 0.82 ± 0.13 for the AP5 group, which is a 57% reduction ($P < 0.01$). This change in the AMPAR/NR current amplitude ratio suggests a change in the currents at the individual synapses of retinal and cortical terminals. This method cannot determine which of the two receptor currents are changing nor does it say whether there have been changes in the number of synapses following NR blockade.

Spontaneous currents reveal increased NR function

To address these issues and to further characterize the kinetics of the NR current, we examined spontaneous (s)EPSCs in 0 mM Mg²⁺ and BMI. These currents are mixed AMPAR and NR currents of both afferent and locally arborizing axons. After an initial period recording the mixed sEPSCs, addition of AP5 was used to isolate the AMPA contribution to sEPSCs. Spontaneous currents were measured in a total of 25 cells from 19 L-AP5-treated and 29 cells from 23 AP5-treated pups, and these neurons are all presented in the time line histograms (Figs. 2 and 3). Twenty-three of the L-AP5-treated cells and 22 of the AP5-treated neurons were from P13 to P20 pups and were therefore used in the quantitative analysis presented as summary bar graphs (Figs. 2 and 3) and in Table 1.

Spontaneous EPSCs recorded in slices from control and AP5-treated colliculi were of qualitatively similar amplitude and frequency (Fig. 2A, left). The frequency distribution of amplitude for individual spontaneous currents was similar between control and AP5-treated animals (Fig. 2A, right). Previous work has shown that miniature events in the developing sSC are between 8 and 10 pA (Shi et al. 2001). By this criterion

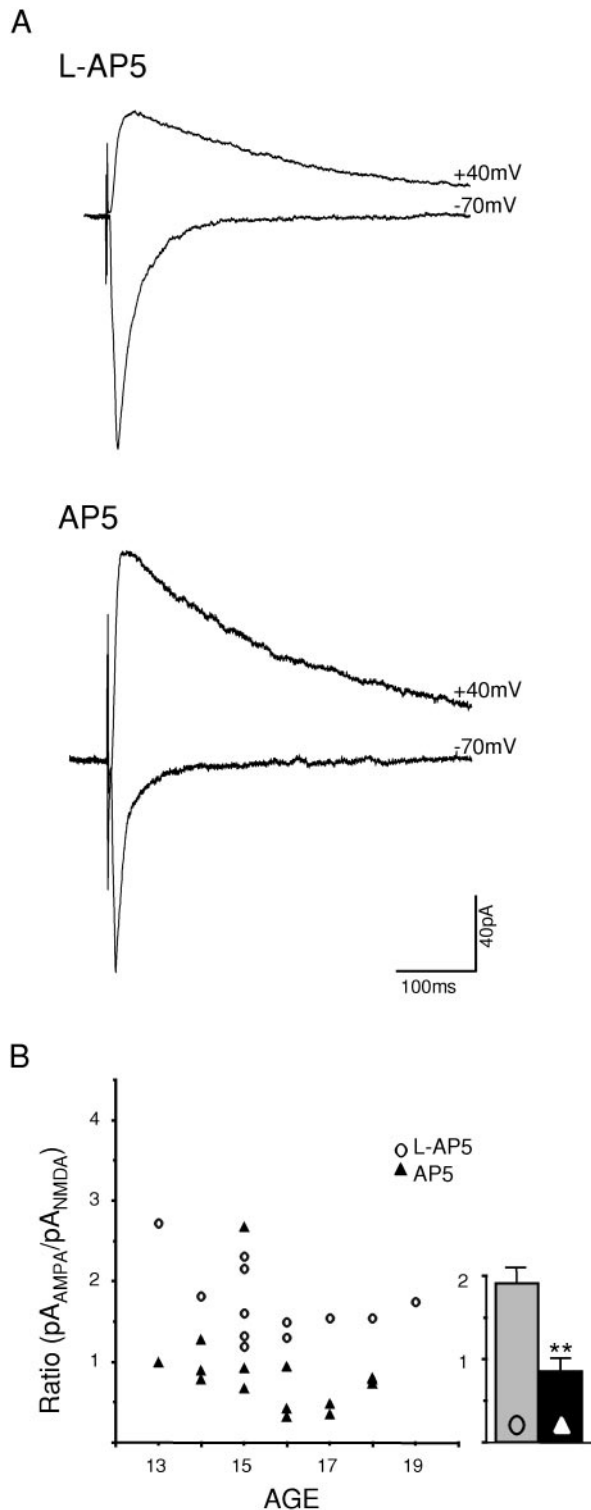


FIG. 1. NMDA receptor (NR) blockade from birth reduces AMPA/kainate receptor (AMPA)/NR current ratios. *A*: excitatory postsynaptic potentials (EPSCs) from superficial superior colliculus (sSC) neurons evoked by stimulation of the stratum opticum are composed of both AMPAR and NR currents [shown here at postnatal day (P)15] in both treatment groups (upward deflection: $+40$ mV with 6μ M BMI and 15μ M GYKI) and AMPAR currents (downward deflection: -70 mV with 6μ M BMI and 50μ M AP5). *B*: ratio of AMPAR to NR current peak amplitude was depressed following (\pm)-2-amino-5-phosphonopentanoic acid (AP5) treatment (closed triangles) compared with L-AP5 controls (open circles) at all ages examined ($P < 0.01$). Each point is the average ratio of 9 evoked EPSCs at each holding potential for a single neuron. Bar graph shows the average current ratio of neurons taken from animals that had opened their eyes (P13–19).

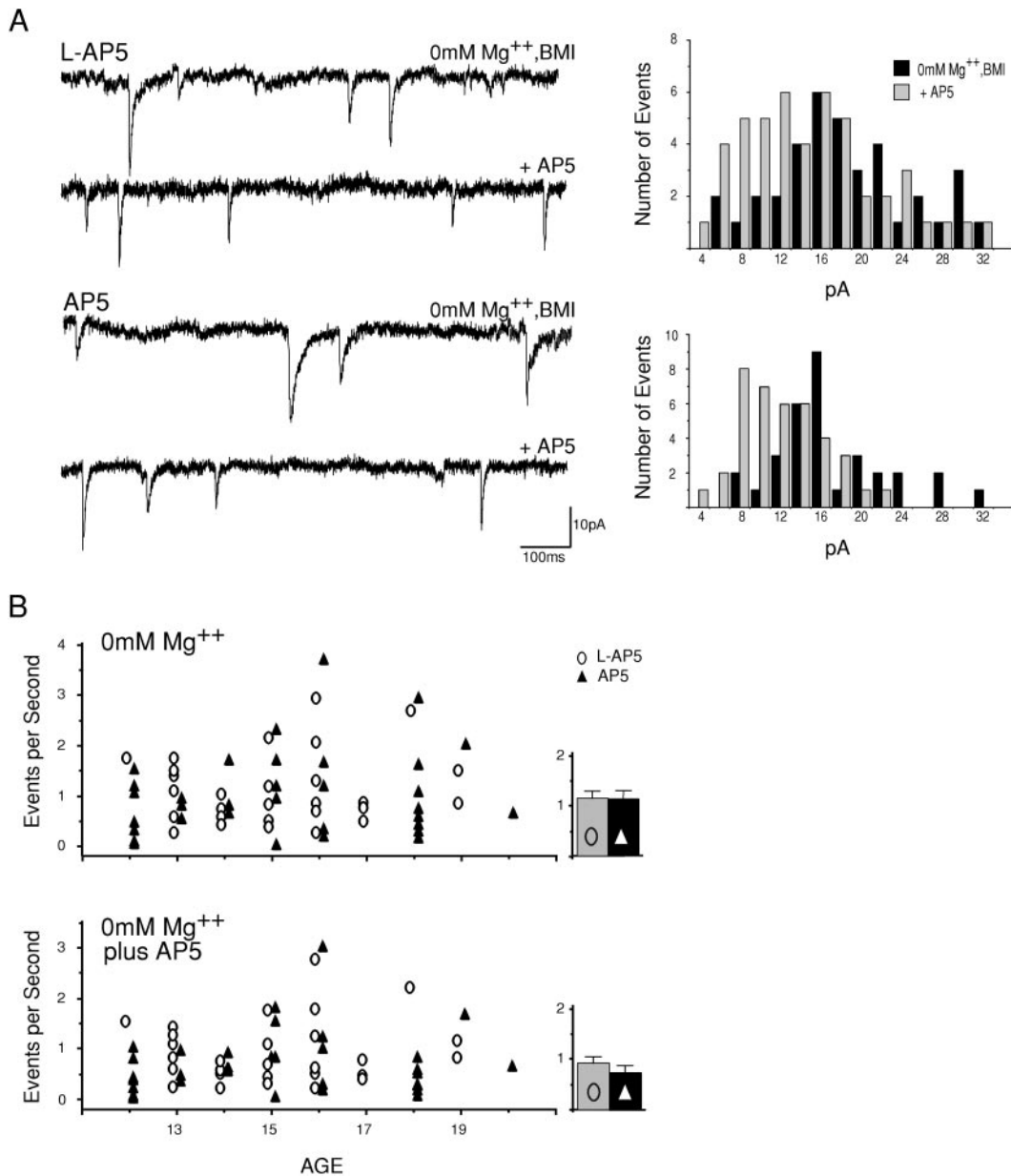


FIG. 2. Spontaneous EPSCs had altered kinetics, but similar frequency following chronic NR blockade. *A, Left*: spontaneous currents from a P16 control (L-AP5)- and a P15 AP5-treated sSC neuron. The slices were maintained in 0 mM Mg²⁺ to relieve the voltage block of NRs. Traces from each cell were taken with both AMPARs and NRs active, and then another was taken with 50 μ M AP5 added to selectively remove NR currents. Current decays that included the NR current were longer in AP5-treated neurons. *Right*: histograms of the peak amplitudes from all the spontaneous events of the neurons shown. Black bars show the distribution of the AMPAR and NR sEPSCs. Gray bars show the isolated AMPAR sEPSC distribution in the same neuron. *B*: scatter plots of sEPSC frequency from control and AP5-treated neurons versus animal age. *Top*: frequency when NRs were active during recording. *Bottom*: Frequency when NRs were inactive. Data show no significant change in the frequency of sEPSCs with age or AP5 treatment. Each point is the number of spontaneous (s)EPSCs per second produced by a single neuron. Bar graphs show the average and SE of the frequency between P13 and P20.

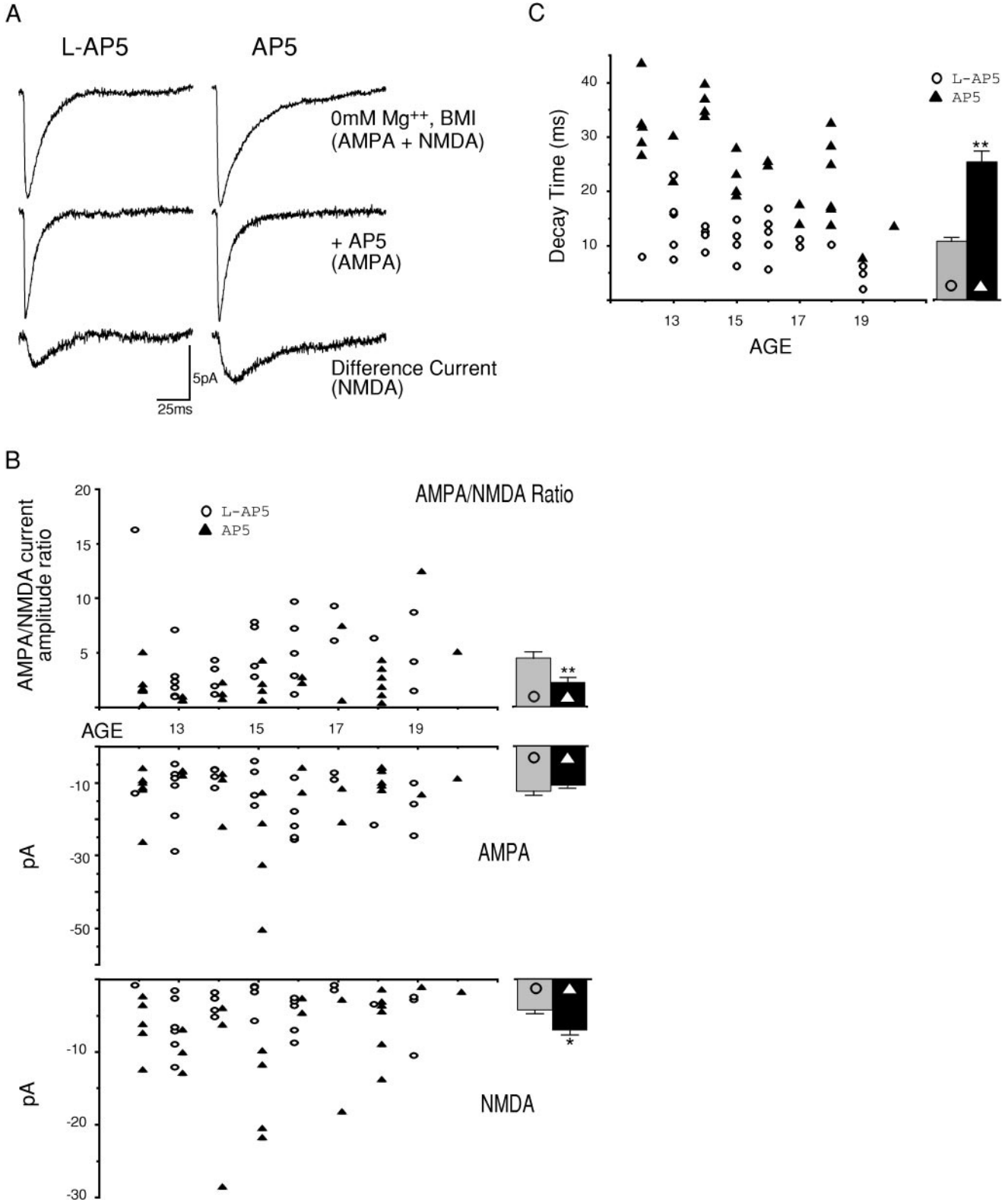
most of the spontaneous events recorded in this study, which clustered around 16 pA, were multiquantal. Addition of NR antagonist to slice perfusate reduced the amplitude of spontaneous currents, probably by increasing the proportion of the miniature events as well as reducing the peak current of multiquantal events. Both the mixed AMPAR/NR sEPSCs and the isolated AMPAR sEPSCs appeared to consist of a similar mix of miniature and multiquantal events in the control and AP5 treatment slices. This suggests that differences between the two

treatment groups do not result from a treatment-induced shift in the prevalence of miniature versus multiquantal events. That there are few events with amplitudes around our cutoff for detection (<4 pA) suggests that we are not missing a large population of synapses in the noise. We can therefore accurately determine a frequency of spontaneous events.

The frequency of sEPSCs is a function of synapse number and the excitability of the intrinsic circuitry within the sSC slice. An induced reduction of synaptic AMPAR current has

previously been demonstrated to be correlated with a decrease in AMPAR sEPSC frequency (Shi et al. 2000). The sEPSC frequency of neurons from AP5-treated colliculi was not different from those of the control colliculi. This was true for both AMPAR sEPSCs and for mixed AMPAR/NR sEPSCs (Table 1; Fig. 2B). Thus, in the week after eye opening, chronic

blockade of NRs did not appear to have a profound effect on the generation of spontaneous intracollicular activity. It appears the AP5 treatment did not cause the emergence of a large number of synapses containing only NRs because the ratio of the sEPSC frequency with the NRs active in the slice to that without them active was similar in both treatment groups.



The chronic NR blockade did not change the frequency of spontaneous currents; however, the currents in neurons from AP5-treated colliculi did have unusually long decay times. This difference was removed when the slice was perfused with AP5, indicating that the longer decay times were the result of altered NR currents (Fig. 2A, left).

To quantitatively examine the amplitude and shape of the NR and AMPAR currents, an average sEPSC was generated for each neuron from the individual sEPSCs of that neuron (Fig. 3A, top trace); this process was then repeated after the addition of AP5 to the perfusate to isolate the AMPAR current (Fig. 3A, middle trace). The average NR current for each neuron was estimated by calculating the difference current that remained after subtracting the AMPAR sEPSC average from the combined AMPAR/NR-mediated current average (see METHODS for details; Fig. 3A, bottom trace).

The peak amplitudes of the average mixed AMPAR/NR sEPSC, the isolated AMPAR current, and NR-mediated difference current were measured for each neuron. An AMPAR/NR peak current amplitude ratio was also calculated for each cell. For both treatment groups, the sEPSC amplitudes were relatively constant across the ages examined (Fig. 3B). To quantify the effects of the AP5 treatment, the sEPSC amplitudes of each neuron between P13 and P20 were averaged together; these data are presented in Table 1. The peak amplitude of the average mixed sEPSCs was not significantly altered by the AP5 treatment. As seen in the evoked currents (Fig. 1), the AMPAR/NR current amplitude ratio of the spontaneous currents was suppressed by AP5 treatment. Thus, even though they may sample different synaptic populations, both the spontaneous and evoked currents showed the same pronounced decrease in the AMPAR/NR current ratio. The average amplitude of spontaneous AMPAR currents was similar between the control and AP5-treated groups. However, the spontaneous NR currents were significantly larger in the AP5-treated neurons. These data indicate that the reduction of the AMPAR/NR sEPSC amplitude ratio with NR blockade was due largely to an increase in the amplitude of NR currents, not a reduction in AMPAR current amplitude.

In normal animals the decay time of NR currents of sSC neurons are subject to two developmental down-regulations: a fast decrease on P11 and a gradual reduction occurring between P8 and P20 (Shi et al. 2000). We examined the necessity of NR currents in driving these events by recording from neurons aged P12 and older. In normal animals, the NR current decay would be substantially shortened at these ages, and only a smaller shortening would be observed during the week after eye opening. As expected, control (L-AP5-treated) pups had short NR current decay times for all ages studied (Fig. 3C,

TABLE 1. Frequency and amplitude of spontaneous synaptic currents after eye opening (P13–20)

	L-AP5	AP5
Frequency (events/s)		
In 0 mM Mg ²⁺ (AMPA and NR active)	1.13 ± 0.17	1.14 ± 0.14
plus AP5 (AMPA active)	0.92 ± 0.12	0.74 ± 0.13
Peak amplitude (pA)		
Combined sEPSC	15 ± 1.70	14.6 ± 1.5
AMPA sEPSC	12.7 ± 1.40	10 ± 1.0
NR difference current	4.1 ± 0.60	6.8 ± 1.2*
AMPA/NR current ratio	4.47 ± 0.59	2.81 ± 0.68†

Values are means ± SE. *n* = 23 L-AP5 and 22 AP5 neurons. *P* values generated by Student's *t*-test. * *P* < 0.05. † *P* < 0.01. AMPA, AMPA/kainate receptor; NR, *N*-methyl-D-aspartate receptor; AP5, (+/-)-2-amino-5-phosphonopentanoic acid; sEPSC, spontaneous excitatory postsynaptic potentials.

Table 2), indicating that the P11 down-regulation has occurred normally. We observed a slight downward trend in the NR decay time of control neurons between P13 and P19 (Fig. 3C), but, when grouped into young and old, this decrease was not significant (Table 2, *P* > 0.05). This failure to find significance is not surprising given the size of the decrease and the few data points available; we have previously been able to observe it in untreated animals with a larger number of data points.

The neurons from sSC chronically treated with AP5 had much longer NR current decay times than L-AP5 controls throughout the observed period (Fig. 3C). This suggests that the P11 down-regulation of NR current decay time did not occur in pups in which the NR had been blocked. The average NR current decay time of all the treated neurons examined after the animals had opened their eyes was 2.5 times longer than the decay times of the NR currents of similarly aged control animals. Averaging over the entire period after eye opening conceals the effect of age on the NR currents of AP5-treated animals, however.

The NR current decay times dropped significantly between P12 and P20 in the treated pups. We quantified this by dividing the neurons along two axes: age and treatment condition (Table 2). For age we used a young group (P12–14) and an old group (P17–20). A two-factor MANOVA showed significant effects of both treatment (*F* = 63.2; *P* < 0.01) and age (*F* = 21.4; *P* < 0.01) as well as an interaction between the two (*F* = 4.3; *P* < 0.05). These statistics support the conclusion that the neurons of young AP5-treated pups have very long NR current decay times initially and that these drop significantly by P17–20. The control neurons, by comparison, show little regulation with age.

This analysis indicates that there is a slow NR-independent

FIG. 3. Average sEPSCs had increased NR current decay times and peak amplitudes following AP5 treatment. *A*: average sEPSCs were computed for each neuron both in the absence (top) and presence (middle) of AP5. Difference currents (bottom), which show the NR contribution to the sEPSC, were computed by subtraction. A neuron from a P15 AP5-treated animal (right) had larger and longer difference currents than one from a control animal (left). The AMPAR currents were of similar amplitude and shape. *B*: peak amplitudes of the average AMPAR and NR sEPSCs, as well as the AMPAR/NR current amplitude ratio, showed an increased contribution of NRs to the sEPSC amplitude. No significant trends of amplitude with age were detected. Histograms beside each scatter plot show the average of all neurons between the ages of P13 and P20. Both the AMPAR/NR current amplitude ratio and the absolute NR current amplitude were significantly larger than control (**P* < 0.05, ***P* < 0.01). *C*: decay time of the average NR sEPSCs was increased until at least P18 by chronic AP5 treatment. L-AP5-treated control neuron decay times (circle) remained short and constant throughout the time examined, while the decay time of AP5- (triangles) treated neurons declined throughout the experimental period. Insufficient data were available to determine whether the apparent convergence of control and treated NR current decay times after P19 is real. Bar graph shows the average decay time of sEPSC currents from P13 to P20, which reveal a significant increase of NR current decay time following AP5 blockade (*t*-test, *P* < 0.01).

TABLE 2. NMDA receptor current decay time

	Young (P12–14)	Old (P17–20)	
L-AP5	12.70 ± 1.52	7.37 ± 1.13	$P > 0.05$
AP5	31.67 ± 1.70	18.68 ± 2.42	$P < 0.01$
	$P < 0.01$	$P < 0.01$	

Values are means ± SE, $n = 6–11$ per group. See METHODS for calculation. P values are by Tukey post-hoc analysis on a two-factor MANOVA (see RESULTS). NMDA, *N*-methyl-D-aspartate.

down-regulation of the NR current decay time active between P12 and P20. However, this NR-independent reduction in decay time is not sufficient to completely compensate for the loss of the P11, calcineurin-mediated down-regulation. Thus NR currents appear to exert a strong feedback effect in down-regulating their own decay time. This feedback role is strongest in the later half of the second postnatal week.

Together the spontaneous and evoked EPSC data indicate that NR blockade has a strong effect on the regulation of NR current amplitude and decay time but has little effect on the regulation of AMPAR currents.

No compensation for NR blockade by calcium-permeant AMPARs

In the hippocampus the incorporation of calcium-permeant AMPARs into synapses has been shown to be dependent on the amount of synaptic calcium entry (Liu and Cull-Candy 2000). We consequently asked whether AP5-treated sSC neurons had compensated for the loss of NR-mediated calcium by altering their AMPAR to allow calcium entry. One possible way this could be accomplished is by excluding the calcium-impermeant forms of the glutamate receptor (GluR 2, 5, 6) (Dingledine et al. 1992) from the synapse. Calcium-permeable AMPARs show inward rectification in the presence of intracellular spermine (Bowie and Mayer 1995; Laezza et al. 1999). We therefore determined the current-voltage curves of the evoked AMPAR EPSCs with spermine in our recording electrode. To prevent postmortem changes, the brain was removed, sectioned, and incubated in 25 μ M AP5 at all times, which is the lowest estimated concentration produced by the Elvax treatment *in vivo*. We did not observe any rectification (Fig. 4) in any of the seven cells studied in this way (4 neurons total from a P12 and a P14 AP5-treated pup, and 3 neurons from a control P13 pup). Thus the widespread appearance of calcium-permeant AMPARs following chronic NMDA blockade is unlikely. In addition, the measured AMPAR currents were not qualitatively different from those reported in the previous experiments, in which NRs were not blocked during slice preparation. Therefore it is unlikely we observed normal AMPAR currents in treated slices simply because they have recovered from a severe depression during the period between slicing and recording.

Protein composition of the synapse is normal following chronic NR blockade

Previous data have indicated that the amount of NR1 mRNA is reduced following chronic AP5 treatment (Hofer et al. 1994). Furthermore, the normal localization of CAMKII in the membrane fraction is disrupted by chronic NR blockade (Scheetz et

al. 1996). Consequently, we wanted to characterize levels of glutamate receptor-related synaptic proteins following the AP5 treatment. Synaptoneuroosomes and whole lysates were prepared from AP5- and L-AP5-treated littermates at P12 (2 isolations from 2 litters) and P16 (3 isolations from 3 litters). Protein concentrations in both fractions were examined by Western blotting for glutamate receptor subunits NR1, NR2A, NR2B, GluR1, and GluR2. Tissue isolated from P16 animals was also probed for proteins known to be associated with the postsynaptic density: Post Synaptic Density Protein 95 (PSD-95), cadherins, Neuronal Cell Adhesion Molecule (NCAM 180 and 140 Kd), calcineurin α , β -catenin, β 3-integrin, and the ephrin receptor EphB2 (Fig. 5). We first characterized the synaptoneurosome fractionation at P16. At this age synaptoneuroosomes prepared from sSC enrich strongly for some postsynaptic proteins (GluR1 and NR2A), but not as much for

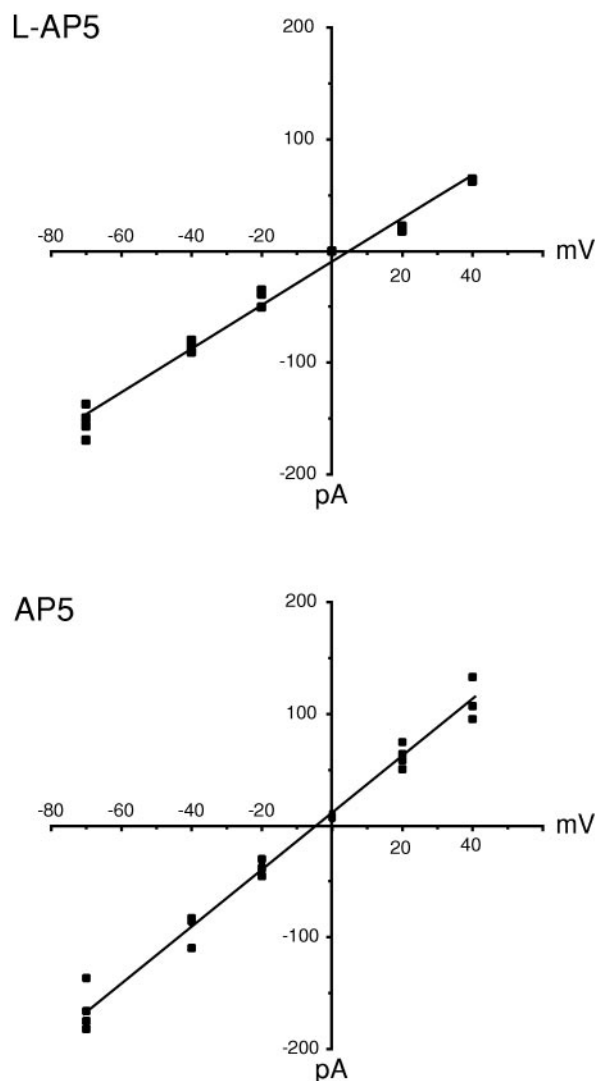


FIG. 4. No rectification of AMPAR currents following NR blockade. In the presence of intracellular spermine and extracellular bicuculline methiodide (BMI) and AP5, current voltage curves were constructed from evoked EPSCs in a single P13 control (L-AP5) and P12 NR-blocked (AP5) neuron. In neither case, nor in any other neurons examined, was there evidence of rectification indicative of calcium-permeant AMPA receptors. Both groups were constantly bathed in 25 μ M AP5 from the time the sSC was dissected to prevent changes at the synapse during the postdissection incubation of the slice.

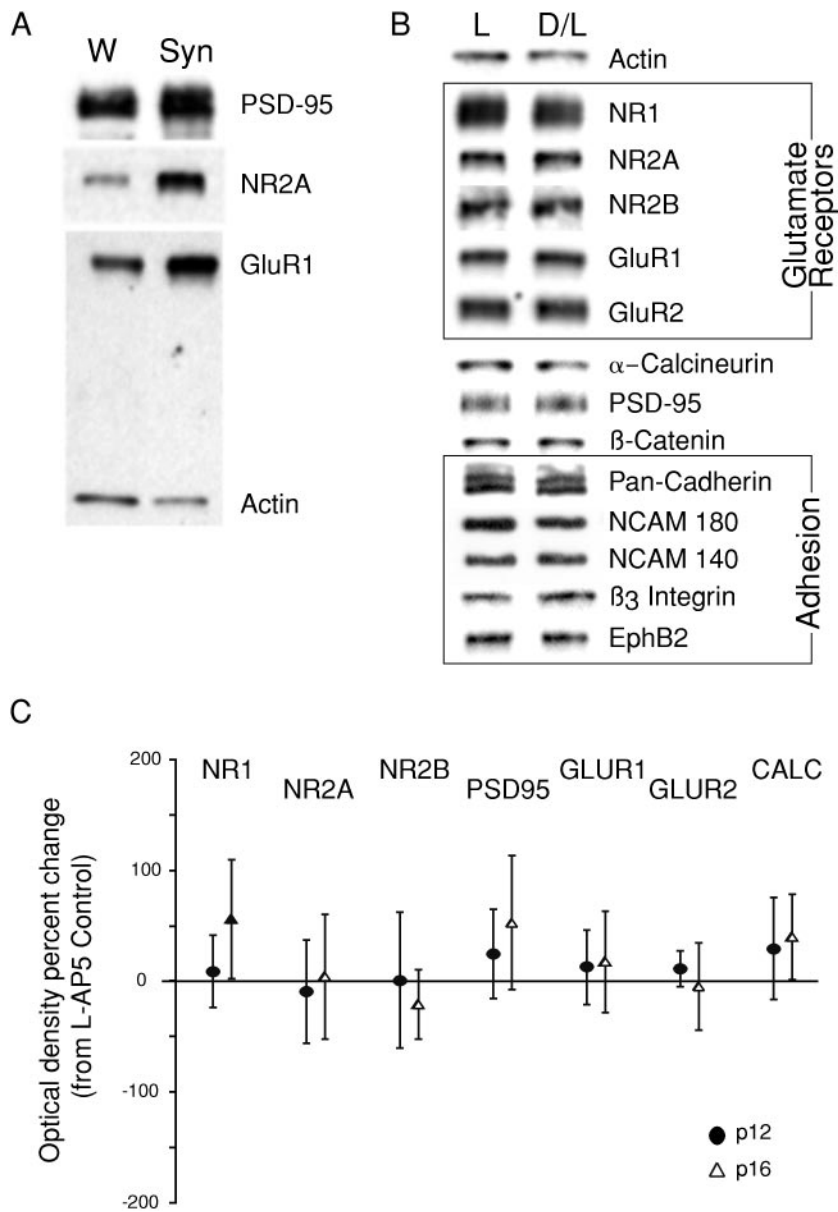


FIG. 5. Western blot analyses of P12 and P16 sSC synaptoneurosomes indicate that synaptic protein composition was normal following NR blockade. *A*: synaptoneurosomes from P16 sSC strongly enrich for some, but not all synaptic proteins. Equal protein amounts of whole (W) lysates and synaptoneurosomes (Syn) preparations showed strong enrichment for NR2A and GluR1 but less for PSD-95. *B*: synaptoneurosomes from P16 sSC showed no difference between L-AP5- (L) or AP5- (D/L) treated sSC for many glutamate receptor subunits (*top*), postsynaptic density associated signaling proteins, or adhesion proteins (*bottom*), indicating that the localization of these proteins to the dendritic fraction can occur in the absence of NR activity. Actin was used as a loading control for all blots. *C*: quantification of optical density of Western blot bands for selected synaptic proteins at P12 and P16. Graph depicts the average percentage change of the optical density of protein bands from AP5-treated sSC relative to their L-AP5-treated littermate controls. Bars indicate the 95% confidence intervals. By this criterion NR1 and calcineurin were slightly elevated in AP5-treated tissue at the $P < 0.05$ level, though these changes were not seen at P12.

others (PSD-95) (Fig. 5A). We did not observe any major differences in the concentration or localization of any of the proteins examined in either whole homogenates (data not shown) or synaptoneurosomes following AP5 treatment at either P16 (Fig. 5B) or P12 (not shown). We tested for subtle changes in the composition of glutamate receptor subunits, PSD-95, and calcineurin in the synaptoneurosomes by quantitatively analyzing differences in the optical density of protein bands on immunoblots between AP5-treated and control (Fig. 5C). Of the proteins NR1, NR2A, NR2B, GluR1, GluR2, PSD95, and calcineurin, only two were elevated beyond their 95% confidence interval: NR1 and calcineurin. These were higher only at P16, and not at all elevated at P12. Thus these data suggest that chronic NR blockade does not produce a consistent change in the levels of glutamate receptor or other synapse-associated proteins in a synaptically enriched cellular fraction of the sSC. This immunoblot data, however, cannot distinguish between levels of protein at functional syn-

apses compared with subsynaptic and nonsynaptic dendritic compartments.

DISCUSSION

The NR has been proposed to be the first receptor to appear during synaptogenesis (Baba et al. 2000; Durand et al. 1996; Isaac et al. 1997; Petralia et al. 1999; Wu et al. 1996) and may be responsible for the maturation of the AMPAR component of the fast excitatory current (Zhu et al. 2000). We have examined the glutamate currents of collicular neurons in slices from animals in which the NR current was pharmacologically blocked from birth. Our data indicate that, in the sSC, blockade of NRs in vivo does not affect the amplitude, frequency, or calcium permeability of AMPAR currents. It is important to note that the blockade of NRs was initiated at the day of birth, 5 to 6 days before spontaneous activity can be detected in the intact animal (Molotchnikoff and Itaya 1993) or in slices (Shi et al. 2000). We do not believe that the apparently normal

AMPA currents of AP5-treated neurons are due to their rapid recovery during the time between cutting and recording, because AP5-treated cells that were maintained in AP5 during cutting and recovery also showed normal AMPA currents. In contrast to the AMPA currents, NR currents are strongly affected by the chronic blockade. They fail to demonstrate the down-regulation of decay time that normally occurs between P10 and P11, and, furthermore, they show an increased peak amplitude.

Activity-dependent modulation of NR current decay time

A decrease in NR current decay time with maturity has been described in many regions of the CNS (Carmignoto and Vicini 1992; Hestrin 1992; Takahashi et al. 1996). This decrease appears to be correlated with the appearance of NR2A subunits (Flint et al. 1997; Takahashi et al. 1996), and this expression of NR2A is increased by activity (Quinlan et al. 1999; Vallano et al. 1996). This process also occurs in the sSC, where the gradual incorporation of NR2A is temporally correlated with a slow reduction of NR decay times that occurs between P8 and P20 (Shi et al. 2000). However, in this neuropil, a rapid, nearly 50% decrease in NR current decay time occurs between P10 and P11. This down-regulation is superimposed on the slower decrease in decay time that correlates with increasing expression of NR2A. The rapid change in the NR current is mediated by the Ca^{2+} /calmodulin-dependent phosphatase calcineurin. This change is inducible in vitro by relatively low-frequency stimulation of sSC afferents. This in vitro induction of the NR current decay time decrease can be blocked either by acute application of AP5 or by voltage clamping stimulated neurons at -70 mV, suggesting that the activity of the NR itself is necessary (Shi et al. 2000). The present data indicate that blockade of the NR in vivo also eliminates the P10–11 calcineurin-dependent drop in NR current decay time. This failure to down-regulate occurs despite the fact that, as a result of the constitutive addition of AMPARs, the overall excitability of the tissue appears normal. The emergence of fast NR currents by P19 and the apparently normal levels of expression of NR2A subunit protein at P12 and P16 indicate that incorporation of the NR2A subunit into synaptic receptors is not perturbed by the NR activity blockade. Lieberman and Mody (1994) have suggested that the localization of calcineurin adjacent to the cytoplasmic face of the NR current pore may constitute a sensitive mechanism for the homeostatic regulation of NR-mediated calcium. The current data are a confirmation of that hypothesis. Our data also support a suggestion from our earlier work that, in the sSC, the P11 down-regulation of the NR current decay time is much more sensitive to NR activity in the neuropil than is the incorporation of the NR2A subunit into synaptic receptors (Shi et al. 2001). Quinlan et al. (1999) have indicated that NR2A levels in synaptoneuroosomes of rat visual cortex rise rapidly with eye opening after dark rearing. Our data showing no difference in NR2A levels after eye opening in AP5-treated compared with control sSC synaptoneuroosomes suggest that, in the sSC, much of the NR2A subunit up-regulation with increasing activity observed after eye opening is independent of current through the NR.

In addition to preventing the P10–11 down-regulation of decay time, chronic NR blockade produced a large increase in the amplitude of NR synaptic currents that was likely respon-

sible for much of the observed decrease in the AMPAR/NR current amplitude ratio. Our immunoblot data showing some up-regulation of NR1, the obligate subunit for NRs, might suggest that the increase reflects a net addition of receptors to each synapse. However, NR2 subunits do not show any increase with AP5 treatment. Therefore the detected increase in NR currents could equally depend on increased cell surface expression of the receptor or on an activity-dependent phosphorylation of the receptor protein (Wang et al. 1996). An up-regulation of NRs by chronic antagonist treatment has been previously demonstrated in tissue culture with receptor binding autoradiography, indicating an increase in surface receptor number (McDonald et al. 1990; Williams et al. 1992). The present observations add the significant information that a similar up-regulation occurs at synaptic receptors. Furthermore, our data on the evoked current ratio provide confirmation that the slow-release plastic, initially applied at P0, is still releasing antagonist in concentrations sufficient to maintain up-regulation of NR expression as late as P18.

AMPA current regulation during development

In the frog tectum (Wu et al. 1996), rat hippocampus (Durand et al. 1996; Zhu et al. 2000), and rat neocortex (Isaac et al. 1997), calcium entry through the NR can convert early glutamate synapses consisting solely of NR currents into synapses expressing AMPARs. This, and a wealth of data on long-term potentiation, have led to the suggestion that the normal maturation of AMPAR currents is initiated by the calcium flux through NRs. However, mice lacking the obligate NR subunit NR1 (Meguro et al. 1992; Monyer et al. 1992) still show some AMPAR currents (Li et al. 1994), as do dissociated neuron cultures grown from these knockouts (Okabe et al. 1998). Recently, hippocampal slice cultures have been shown to overcome an initial delay in AMPAR development after a few days of chronic treatment with AP5 (Zhu and Malinow 2002). It was suggested that this reflects a compensatory mechanism triggered by the persistent absence of NR activity. These previous studies and the current data could also be the result of constitutive AMPAR insertion that occurs with a much slower time course than the rapid up- and down-titration of AMPAR currents mediated by NR activity. Regardless of the mechanism involved, these studies all indicate that AMPAR currents can develop in the absence of NR currents. The present results add to previous work in showing that, in vivo, the amplitude and frequency of AMPAR currents can attain levels that are indistinguishable from normal animals even when NRs are blocked throughout the majority of synaptogenesis. However, these data do not necessarily imply that AMPAR current development is normally independent of NR currents. Considerable data in the hippocampus and the neocortex suggest that NR function can depress as well as potentiate AMPAR function; similar bidirectional control has been detected in the amphibian homologue of the sSC, the optic tectum (Zhang et al. 1998). Moreover, in the postnatal rat sSC, we have previously shown that chronic treatment with low levels of NMDA itself can depress AMPAR currents, probably because the treatment partially desensitizes NRs, resulting in constant weak NR activation.

Therefore we favor a model of glutamate synapse development in which AMPAR development can proceed in the absence of the NR, though under normal circumstances the NR serves to modulate AMPAR currents at individual synapses. It

is possible, though not directly shown by our results, that NR-independent mechanisms normally regulate synaptic strength and that these NR-independent processes work in addition to or in concert with the NR-dependent regulation during normal development. What is unique about the NR-dependent mechanism is that it determines which synapses are depressed and withdrawn and which are reinforced and retained. Consistent with this are numerous observations that the distribution of axon terminals as well as the local elaboration of developing dendrites are abnormal when the NR is disrupted in early development (Huang and Pallas 2001; Iwasoto et al. 2000; Simon et al. 1992).

We have little evidence regarding the nature of the NR-independent developmental regulation, but several studies have now documented a robust, NR-independent regulation of glutamatergic function in tissue culture neurons grown with varying levels of activity (O'Brien et al. 1998; Turrigiano et al. 1998). One distinguishing characteristic of at least one form of this homeostasis is that both the AMPAR and NR currents are coregulated to maintain a constant AMPAR/NR current ratio (Watt et al. 2000). Developing synapses must operate at widely different activity levels as the brain matures, and so it is attractive to extrapolate this scaling system to them. The current data suggest, however, that scaling may be much more complex in the intact developing brain, because we show that AMPAR and NR receptor levels can be regulated independently of each other.

In addition to demonstrating separable systems of developmental regulation between the NRs and the AMPARs, the current data provide insight on several previously documented disruptions of synaptic differentiation arising from the same NR block. For example, in addition to the CaN-dependent down-regulation of NR current decay time documented here, the same chronic AP5 treatment has been shown to decrease the up-regulation of NR1 transcripts during the second postnatal week (Hofer et al. 1994); disrupt the localization of CaMKII protein (Scheetz et al. 1996); eliminate or delay the completion of map refinement (Simon et al. 1992); and facilitate sprouting of the ipsilateral retinocollicular projection (Colonnese and Constantine-Paton 2001). Our present data suggest that these disruptions are likely to arise specifically from the absence of NR function and not from a general depression of excitatory synaptic transmission.

There are also several developmental events that seem to proceed normally in NR blocked sSC. For example, competition between the inputs from the two retinas and the visual cortical projection for vacated synaptic space occurs in AP5-treated sSC (Colonnese and Constantine-Paton, 2001). The normal levels of most of the synapse-related proteins we have examined in this study represent a second group of processes for which the NR current is not required. If fast glutamatergic activity is involved in these processes at all, then they are tied to AMPAR, kainate, and metabotropic receptors and not directly to signaling through the NR channel.

We thank Dr. Michael Greenberg for the kind gift of the EphB2 antibody.

This work was supported by National Eye Institute Grant EY-06039 and EY-104074, formerly NS-32290 to M. Constantine-Paton.

REFERENCES

- Baba H, Doubell TP, Moore KA, and Woolf CJ.** Silent NMDA receptor-mediated synapses are developmentally regulated in the dorsal horn of the rat spinal cord. *J Neurophysiol* 83: 955–962, 2000.
- Bowie D and Mayer ML.** Inward rectification of both AMPA and kainate subtype glutamate receptors generated by polyamine-mediated ion channel block. *Neuron* 15: 453–462, 1995.
- Carmignoto G and Vicini S.** Activity-dependent decrease in NMDA receptor responses during development of the visual cortex. *Science* 258: 1007–1011, 1992.
- Carroll RC, Lissin DV, von Zastrow M, Nicoll RA, and Malenka RC.** Rapid redistribution of glutamate receptors contributes to long-term depression in hippocampal cultures. *Nat Neurosci* 2: 454–460, 1999.
- Chen C and Regehr WG.** Developmental remodeling of the retinogeniculate synapse. *Neuron* 28: 955–966, 2000.
- Cline HT and Constantine-Paton M.** NMDA receptor antagonists disrupt the retinotectal topographic map. *Neuron* 3: 413–426, 1989.
- Colonnese MT and Constantine-Paton M.** Chronic NMDA receptor blockade from birth increases the sprouting capacity of ipsilateral retinocollicular axons without disrupting their early segregation. *J Neurosci* 21: 1557–1568, 2001.
- Constantine-Paton M, Cline HT, and Debski E.** Patterned activity, synaptic convergence, and the NMDA receptor in developing visual pathways. *Annu Rev Neurosci* 13: 129–154, 1990.
- Dingledine R, Hume RI, and Heinemann SF.** Structural determinants of barium permeation and rectification in non-NMDA glutamate receptor channels. *J Neurosci* 12: 4080–4087, 1992.
- Durand GM, Kovalchuk Y, and Konnerth A.** Long-term potentiation and functional synapse induction in developing hippocampus. *Nature* 381: 71–75, 1996.
- Fagni L, Chavis P, Ango F, and Bockaert J.** Complex interactions between mGluRs, intracellular Ca^{2+} stores and ion channels in neurons. *Trends Neurosci* 23: 80–88, 2000.
- Flint AC, Maisch US, Weishaupt JH, Kriegstein AR, and Monyer H.** NR2A subunit expression shortens NMDA receptor synaptic currents in developing neocortex. *J Neurosci* 17: 2469–2476, 1997.
- Fox K, Schlaggar BL, Glazewski S, and O'Leary DD.** Glutamate receptor blockade at cortical synapses disrupts development of thalamocortical and columnar organization in somatosensory cortex. *Proc Natl Acad Sci USA* 93: 5584–5589, 1996.
- Groc L, Gustafsson B, and Hanse E.** Spontaneous unitary synaptic activity in CA1 pyramidal neurons during early postnatal development: constant contribution of AMPA and NMDA receptors. *J Neurosci* 22: 5552–5562, 2002.
- Hahn JO, Langdon RB, and Sur M.** Disruption of retinogeniculate afferent segregation by antagonists to NMDA receptors. *Nature* 351: 568–570, 1991.
- Hestrin S.** Developmental regulation of NMDA receptor-mediated synaptic currents at a central synapse. *Nature* 357: 686–689, 1992.
- Heynen AJ, Quinlan EM, Bae DC, and Bear MF.** Bidirectional, activity-dependent regulation of glutamate receptors in the adult hippocampus in vivo. *Neuron* 28: 527–536, 2000.
- Hickmott PW and Constantine-Paton M.** Experimental down-regulation of the NMDA channel associated with synapse pruning. *J Neurophysiol* 78: 1096–1107, 1997.
- Hofer M, Prusky GT, and Constantine-Paton M.** Regulation of NMDA receptor mRNA during visual map formation and after receptor blockade. *J Neurochem* 62: 2300–2307, 1994.
- Hollingsworth EB, McNeal ET, Burton JL, Williams RJ, Daly JW, and Creveling CR.** Biochemical characterization of a filtered synaptoneurosome preparation from guinea pig cerebral cortex: cyclic adenosine 3':5'-monophosphate-generating systems, receptors, and enzymes. *J Neurosci* 5: 2240–2253, 1985.
- Hohnke CD, Oray S, and Sur M.** Activity-dependent patterning of retinogeniculate axons proceeds with a constant contribution from AMPA and NMDA receptors. *J Neurosci* 20: 8051–8060, 2000.
- Huang L and Pallas SL.** NMDA antagonists in the superior colliculus prevent developmental plasticity but not visual transmission or map compression. *J Neurophysiol* 86: 1179–1194, 2001.
- Isaac JT, Crair MC, Nicoll RA, and Malenka RC.** Silent synapses during development of thalamocortical inputs. *Neuron* 18: 269–280, 1997.
- Iwasato T, Datwani A, Wolf AM, Nishiyama H, Taguchi Y, Tonegawa S, Knopfel T, Erzurumlu RS, and Itohara S.** Cortex-restricted disruption of NMDAR1 impairs neuronal patterns in the barrel cortex. *Nature* 406: 726–731, 2000.
- Iwasato T, Erzurumlu RS, Huerta PT, Chen DF, Sasaoka T, Ulupinar E, and Tonegawa S.** NMDA receptor-dependent refinement of somatotopic maps. *Neuron* 19: 1201–1210, 1997.

- Laezza F, Doherty JJ, and Dingledine R.** Long-term depression in hippocampal interneurons: joint requirement for pre- and postsynaptic events. *Science* 285: 1411–1414, 1999.
- Li Y, Erzurumlu RS, Chen C, Jhaveri S, and Tonegawa S.** Whisker-related neuronal patterns fail to develop in the trigeminal brainstem nuclei of NR1 knockout mice. *Cell* 76: 427–437, 1994.
- Lieberman DN and Mody I.** Regulation of NMDA channel function by endogenous Ca(2+)-dependent phosphatase. *Nature* 369: 235–239, 1994.
- Liu SQ and Cull-Candy SG.** Synaptic activity at calcium-permeable AMPA receptors induces a switch in receptor subtype. *Nature* 405: 454–458, 2000.
- Lo FS and Mize RR.** Synaptic regulation of L-type Ca(2+) channel activity and long-term depression during refinement of the retinocollicular pathway in developing rodent superior colliculus. *J Neurosci* 20: RC58, 2000.
- McDonald JW, Silverstein FS, and Johnston MV.** MK-801 pretreatment enhances N-methyl-D-aspartate-mediated brain injury and increases brain N-methyl-D-aspartate recognition site binding in rats. *Neuroscience* 38: 103–113, 1990.
- Meguro H, Mori H, Araki K, Kushiya E, Kutsuwada T, Yamazaki M, Kumanishi T, Arakawa M, Sakimura K, and Mishina M.** Functional characterization of a heteromeric NMDA receptor channel expressed from cloned cDNAs. *Nature* 357: 70–74, 1992.
- Miyamoto T and Okada Y.** NMDA receptor, protein kinase C and calmodulin system participate in the long-term potentiation in guinea pig superior colliculus slices. *Brain Res* 605: 287–292, 1993.
- Molotchnikoff S and Itaya SK.** Functional development of the neonatal rat retinotectal pathway. *Brain Res Dev Brain Res* 72: 300–304, 1993.
- Monyer H, Sprengel R, Schoepfer R, Herb A, Higuchi M, Lomeli H, Burnashev N, Sakmann B, and Seeburg PH.** Heteromeric NMDA receptors: molecular and functional distinction of subtypes. *Science* 256: 1217–1221, 1992.
- O'Brien RJ, Kamboj S, Ehlers MD, Rosen KR, Fischbach GD, and Hagan RL.** Activity-dependent modulation of synaptic AMPA receptor accumulation. *Neuron* 21: 1067–1078, 1998.
- Okabe S, Vicario-Abejon C, Segal M, and McKay RD.** Survival and synaptogenesis of hippocampal neurons without NMDA receptor function in culture. *Eur J Neurosci* 10: 2192–2198, 1998.
- Petralia RS, Esteban JA, Wang YX, Partridge JG, Zhao HM, Wenthold RJ, and Malinow R.** Selective acquisition of AMPA receptors over postnatal development suggests a molecular basis for silent synapses. *Nat Neurosci* 2: 31–36, 1999.
- Prusky GT and Ramoa AS.** Novel method of chronically blocking retinal activity. *J Neurosci Methods* 87: 105–110, 1999.
- Quinlan EM, Olstein DH, and Bear MF.** Bidirectional, experience-dependent regulation of N-methyl-D-aspartate receptor subunit composition in the rat visual cortex during postnatal development. *Proc Natl Acad Sci USA* 96: 12876–12880, 1999.
- Scheetz AJ, Nairn AC, and Constantine-Paton M.** NMDA receptor-mediated control of protein synthesis at developing synapses. *Nat Neurosci* 3: 211–216, 2000.
- Scheetz AJ, Prusky GT, and Constantine-Paton M.** Chronic NMDA receptor antagonism during retinotopic map formation depresses CaM kinase II differentiation in rat superior colliculus. *Eur J Neurosci* 8: 1322–1328, 1996.
- Schlaggar BL, Fox K, and O'Leary DD.** Postsynaptic control of plasticity in developing somatosensory cortex. *Nature* 364: 623–626, 1993.
- Shi J, Aamodt SM, and Constantine-Paton M.** Temporal correlations between functional and molecular changes in NMDA receptors and GABA neurotransmission in the superior colliculus. *J Neurosci* 17: 6264–6276, 1997.
- Shi J, Aamodt SM, Townsend M, and Constantine-Paton M.** Developmental depression of glutamate neurotransmission by chronic low-level activation of NMDA receptors. *J Neurosci* 21: 6233–6244, 2001.
- Shi J, Townsend M, and Constantine-Paton M.** Activity-dependent induction of tonic calcineurin activity mediates a rapid developmental downregulation of NMDA receptor currents. *Neuron* 28: 103–114, 2000.
- Shi SH, Hayashi Y, Petralia RS, Zaman SH, Wenthold RJ, Svoboda K, and Malinow R.** Rapid spine delivery and redistribution of AMPA receptors after synaptic NMDA receptor activation. *Science* 284: 1811–1816, 1999.
- Simon DK, Prusky GT, O'Leary DD, and Constantine-Paton M.** N-methyl-D-aspartate receptor antagonists disrupt the formation of a mammalian neural map. *Proc Natl Acad Sci USA* 89: 10593–10597, 1992.
- Smith AL, Cordery PM, and Thompson ID.** Manufacture and release characteristics of Elvax polymers containing glutamate receptor antagonists. *J Neurosci Methods* 60: 211–217, 1995.
- Takahashi T, Feldmeyer D, Suzuki N, Onodera K, Cull-Candy SG, Sakimura K, and Mishina M.** Functional correlation of NMDA receptor epsilon subunits expression with the properties of single-channel and synaptic currents in the developing cerebellum. *J Neurosci* 16: 4376–4382, 1996.
- Turrigiano GG, Leslie KR, Desai NS, Rutherford LC, and Nelson SB.** Activity-dependent scaling of quantal amplitude in neocortical neurons. *Nature* 391: 892–896, 1998.
- Vallano ML, Lambolez B, Audinat E, and Rossier J.** Neuronal activity differentially regulates NMDA receptor subunit expression in cerebellar granule cells. *J Neurosci* 16: 631–639, 1996.
- Wallace H, Glazewski S, Liming K, and Fox K.** The role of cortical activity in experience-dependent potentiation and depression of sensory responses in rat barrel cortex. *J Neurosci* 21: 3881–3894, 2001.
- Wang YT, Yu XM, and Salter MW.** Ca(2+)-independent reduction of N-methyl-D-aspartate channel activity by protein tyrosine phosphatase. *Proc Natl Acad Sci USA* 93: 1721–1725, 1996.
- Watt AJ, van Rossum MC, MacLeod KM, Nelson SB, and Turrigiano GG.** Activity coregulates quantal AMPA and NMDA currents at neocortical synapses. *Neuron* 26: 659–670, 2000.
- Williams K, Dichter MA, and Molinoff PB.** Up-regulation of N-methyl-D-aspartate receptors on cultured cortical neurons after exposure to antagonists. *Mol Pharmacol* 42: 147–151, 1992.
- Wu G, Malinow R, and Cline HT.** Maturation of a central glutamatergic synapse. *Science* 274: 972–976, 1996.
- Zhang LI, Tao HW, Holt CE, Harris WA, and Poo M.** A critical window for cooperation and competition among developing retinotectal synapses. *Nature* 395: 37–44, 1998.
- Zhu JJ, Esteban JA, Hayashi Y, and Malinow R.** Postnatal synaptic potentiation: delivery of GluR4-containing AMPA receptors by spontaneous activity. *Nat Neurosci* 3: 1098–1106, 2000.
- Zhu JJ and Malinow R.** Acute versus chronic NMDA receptor blockade and synaptic AMPA receptor delivery. *Nat Neurosci* 5: 513–514, 2002.